




---

# EVALUATION OF MACHINE-LEARNING MODELS TO MEASURE INDIVIDUALIZED TREATMENT EFFECTS FROM RANDOMIZED CLINICAL TRIAL DATA WITH TIME-TO-EVENT OUTCOMES

---

 **Elvire Roblin**  
MICS, CentraleSupélec  
Oncostat CESP U1018, Inserm,  
Université Paris-Saclay, France

 **Paul-Henry Cournède**  
MICS, CentraleSupélec,  
Université Paris-Saclay,  
Gif-sur-Yvette, France

 **Stefan Michiels**  
Oncostat CESP U1018, Inserm,  
Université Paris-Saclay,  
Villejuif, France

## ABSTRACT

In randomized clinical trials, regression models can be used to explore the relationships between patients' variables (e.g., clinical, pathological or lifestyle variables, and also biomarker or genomics data) and the magnitude of treatment effect. Our aim is to evaluate the value of flexible machine learning models that can incorporate interactions and nonlinear effects of high-dimensional data to estimate individualized treatment recommendations in the setting of such trials with time-to-event outcomes. We compare survival models based on neural networks (CoxCC and CoxTime) and random survival forests (Interaction Forests). A Cox model, including an adaptive LASSO penalty, is used as a benchmark. Specific metrics for individualized treatment recommendations are used: the C-for-Benefit, the E50-for-Benefit, and RMSE for treatment benefit. We conduct an extensive simulation study using 2 different data generation processes incorporating nonlinearity and interactions up to the third order. The models are applied to gene expression and clinical data from 2 breast cancer studies. The machine learning-based methods show reasonable performances on the simulation data sets, especially in terms of discrimination for Interaction Forests and calibration for the neural networks. They can be used to evaluate individualized treatment effects from randomized trials when nonlinear and interaction effects are expected to be present.

**Keywords** Randomized Control Trial, Feedforward Neural Network, Interaction Forest, LASSO, Personalized Medicine, Individualized Treatment Effect

## 1 Introduction

Precision medicine consists of identifying which intervention is likely to be most beneficial for a given patient. It is defined by the European Society for Medical Oncology (Yates et al., 2018) as a "healthcare approach with the primary aim of identifying which interventions are likely to be of most benefit for which patients based upon the features of the individual and their disease". It focuses on characterizing the variability in patients' response to treatment and estimating individualized treatment benefits. In randomized clinical trials (RCTs), in which patients are randomly assigned to two treatment groups: one that receives the experimental treatment, often called the treatment group, and a second group that does not receive the treatment, often called the control group, treatment benefit is typically calculated as an average across the study population. In an RCT, an individual treatment benefit can be defined as the difference in survival outcomes for a given patient at a pre-specified time point with and without the treatment. The assessment of this treatment benefit is based on a counterfactual approach (Rubin, 1974), as both outcomes cannot be observed for a given individual.

In this work, we explore the potential of two families of machine learning methods to estimate individual patient treatment benefits from data in a high-dimensional setting and in the context of an RCT. We apply 2 strategies for the feedforward neural networks (FNNs) based on a specific loss function in a continuous time framework (CoxCC and CoxTime) (Kvamme et al., 2019), and Interaction Forests (IF), an algorithm based on diversity forests that accounts for

bidirectional interactions. We benchmark these methods with a penalized Cox Proportional Hazards (CoxPH) model (Cox, 1972) with an adaptive LASSO penalty, as previously recommended by Ternès et al. (2017).

Our study examines the potential of the methods to estimate individual patient treatment benefit from data in a high-dimensional setting, when non-linear and interaction effects are present. We apply calibration and discrimination measures specifically designed for the potential outcome framework and adapt some of these measures to a time-to-event outcome.

The performances of the different models are evaluated and compared using a simulation study with two different data generation processes. To overcome the linear framework without interactions, we simulate data with nonlinearity and interactions up to the third order. We also present the results on two breast cancer patient data sets with high-dimensional gene expression, evaluating the effect of adding either taxane chemotherapy or trastuzumab to a standard chemotherapy treatment.

## 2 Related work

In an RCT, the analysis focuses on the treatment effect, which refers to the impact of a treatment on a specific outcome variable. This variable can be of various types, such as a binary outcome or time-to-event. Different methods have been suggested to propose a measure of the treatment effect. With the FNN model DeepSurv, Katzman et al. (2018) provide a personalized recommendation method derived from randomized data, which may predict survival in a subgroup of patients. Klaveren et al. (2017) focus on outcome risk and define treatment benefit as the difference between outcome risk with and without therapy. They define treatment benefit in 2 different ways. Observed treatment benefit is the difference in survival outcome between 2 patients with the same predicted benefit but with different treatment assignments. The predicted treatment benefit is the predicted risk with a treatment for a given patient minus the predicted risk with an alternative treatment option for the same patient.

In the counterfactual framework, a matching procedure should be implemented to compute observed treatment benefit. Different methods can create pairs of patients with similar profiles but different treatment assignments. Patients can be matched on predicted benefit (Klaveren et al., 2017): 2 patients are paired if they have close predicted benefit and discordant treatment assignments. Klaveren et al. (2017) compare this procedure with an alternative matching based on covariates. This second matching procedure is also applied by Maas et al. (2023) They use the Mahalanobis distance between patients' characteristics to create pairs of patients.

Klaveren et al. (2017) study binary outcomes and predicted risk, discussing how to extend their measure to time-to-event data. Rekkas et al. (2023) estimate individualized treatment effects from an RCT, comparing various risk-based approaches with a binary outcome. Bouvier et al. (2024) investigate methods for evaluating individualized treatment effects with time-to-event outcomes using individual participant data meta-analysis, highlighting the potential of meta-analysis in predicting individualized treatment outcomes.

## 3 Material and Methods

### 3.1 Notations

Let the random variable  $T \in \mathbb{R}^+$  represent the survival time, that is the time between the starting point and the occurrence of a given event (e.g. the time between a patient's treatment assignment and death). The survival function at time  $t$ ,  $S(t)$ , is defined as:

$$S(t) = P(T > t).$$

The survival function can be obtained through the cumulative hazard  $H(t)$ :

$$S(t) = \exp(-H(t)),$$

with  $H(t) = \int_0^t h(s)ds$ , and  $h(t)$  the hazard rate.  $H_0$  is the cumulative hazard at baseline for time  $t = 0$ .

Often,  $T$  is not observed for all individuals: time-to-event data is censored. Survival data is said to be right-censored if the individual leaves the study before the end point or if the event did not happen before the end of the follow-up. In the case of right-censoring, we define  $(C_i)_{i=1,\dots,n}$  the independent and identically distributed censoring times of  $n$  individuals. We can set  $\{\tilde{T}_i, X_i, D_i\}_{i=1,\dots,n}$  where  $\tilde{T} = \min(T_i, C_i)$  is the time until death or censoring,  $X_i = (X_{i,1}, \dots, X_{i,p})^T \in \mathbb{R}^p$  denotes a  $p$ -dimensional vector of variables, and  $D_i = \mathbb{I}\{\tilde{T}_i = T_i\}$  is the censoring indicator. We suppose that the survival time  $T_i$  is independent of the censoring time conditionally on the variables vector  $X_i$  for  $i = 1, \dots, n$ .  $G(t)$  can be defined as the estimate of the censoring survival function:

$$G(t) = P(C > t).$$

### 3.2 Models

In this paper, we compare 3 survival-adapted machine learning algorithms and investigate their ability to predict treatment effects. More specifically, we compare 2 FNNs that use specific loss functions to handle censored observations with IF, a specific type of random survival forest (RSF) that models interaction effects. These models are benchmarked with a penalized CoxPH with linear effects and the LASSO penalty.

#### 3.2.1 Benchmark method : CoxPH with adaptive LASSO penalty

The Cox Proportional Hazards (CoxPH) model (Cox, 1972) is the most commonly used regression method in survival analysis. In a regression model, the objective is to estimate regression coefficients to assess the strength of association between the predictors  $X$  and the outcome. For a given patient  $i$ , represented by a triplet  $(X_i, \tilde{T}_i, D_i)$ , the hazard function  $h(t, X_i)$  examines how variables influence the rate of a particular event happening at a specific time  $t$ . It is written as:

$$h(t|X_i) = h_0(t) \exp(\beta^T X_i), \text{ for } i = 1, \dots, n, \quad (1)$$

where the baseline hazard function,  $h_0(t)$ , can be an arbitrary non-negative function of time.  $\beta^T = (\beta_1, \dots, \beta_p)$  is the coefficient vector associated with the variables.

This CoxPH model relies on two assumptions. First, it supposes a linear relationship between the log hazard and the variables  $X_i$ , with the baseline hazard being an intercept term that varies with time. Additionally, the ratio of the instantaneous risk for any 2 patients is independent of time  $t$ : this corresponds to the proportional hazard assumption.

With high dimensional data, the model can become non-identifiable. A LASSO penalty can be introduced to select only the variables with the strongest effects on the outcome of interest. First introduced in the context of linear regression by Tibshirani (1996) and then adapted to survival analysis (Tibshirani, 1997), the LASSO penalty corresponds to the  $L_1$  norm of the regression coefficients. The penalization term is denoted by:

$$\text{pen}(\lambda) = \lambda \|\beta\|_1 = \lambda \left( \sum_{j=1}^p |\beta_j| \right).$$

The model's degree of parsimony or complexity depends on the penalization parameter  $\lambda$ : it varies from 0 (complete model including all biomarkers) to  $+\infty$  (null model with no biomarkers).  $\lambda$  is often estimated using cross-validation (CV).

In certain scenarios, LASSO can be inconsistent for variable selection. Here, we implement adaptive lasso (ALASSO) (Fan and Lv, 2008), a method based on an additive penalization term for a more conservative choice of the shrinkage parameter lambda. With ALASSO, adaptive weights are used for penalizing difference coefficients in the  $L_1$  penalty. The penalization term becomes:

$$\text{pen}(\lambda) = \lambda \left( \sum_{j=1}^p w_j |\beta_j| \right), \quad (2)$$

where  $w_j = \frac{1}{|\hat{\beta}_j|}$  are biomarker-specific weights, and  $\hat{\beta}_j, j = 1, \dots, p$  are estimated by fitting a preliminary regular LASSO. The non-negative penalty parameter  $\lambda$  for the adaptive lasso is chosen using the maximum cross-validated log-likelihood method.

#### 3.2.2 Machine learning algorithms adapted to time-to-event outcomes

The hypotheses of the linear CoxPH model are restrictive, for instance, when nonlinear and complex interactions exist in the data. Here, we focus on artificial neural networks and random forests, as these algorithms can model complex patterns.

Kvamme et al. (2019) introduced a method called CoxCC that uses a loss function based on a case-control approximation. They proposed to randomly sample a new set of controls at each iteration instead of keeping control samples fixed. The loss is written as:

$$\mathcal{L}_{\text{CoxCC}} = \frac{1}{n} \sum_{i: D_i=1} \log \left( \sum_{j \in \tilde{\mathcal{R}}_i} \exp[\phi(X_j) - \phi(X_i)] \right), \quad (3)$$

with  $\tilde{\mathcal{R}}_i$  a subset of the risk set  $\mathcal{R}_i$  at time  $t$  including individual  $i$ .  $i$  represents the case, and the  $j$ 's are the controls sampled from the risk set.  $\phi$  represents the transformation operated by the FNN on the input variables. CoxCC can be trained with this specific loss (Equation 3) using a mini-batch gradient descent algorithm.

The authors also developed a second version of their model, CoxTime, that is not constrained by the proportionality assumption. To do so, they added the time variable as an additional input to the model. The loss function can then be rewritten as:

$$\mathcal{L}_{\text{Cox-Time}} = \frac{1}{n} \sum_{i:D_i=1} \log \left( \sum_{j \in \mathcal{R}^i} \exp [\phi(t_i, X_j) - \phi(t_i, X_i)] \right). \quad (4)$$

The FNNs are compared with IF (Hornung and Boulesteix, 2022), a type of random survival forest specifically designed to model quantitative and qualitative interaction effects in bivariate splits. 2 variables are said to interact if the effect of one variable on the outcome depends on the value of the other variable. Here, we focus on biomarker-by-treatment interactions in the setting of an RCT. Two types of interactions are accounted for: the quantitative interactions and the qualitative interactions, as categorized by Peto (1982). For a quantitative interaction, the treatment effect differs quantitatively depending on the biomarker value, but it remains in the same direction conditional on biomarker values (e.g., the treatment effect increases when the biomarker value increases). Conversely, when considering a qualitative interaction, the direction of the treatment effect depends on the biomarker value. As they are based on multivariable splitting, IFs are specifically developed to model these interactions.

### 3.2.3 Hyperparameter search

Specific hyperparameter search procedures are implemented for each machine learning model.

For the FNN models, we perform the hyperparameter search in the context of a 5-fold CV applied on the training set. First, the data is split into a training and a test set. Then the 5-fold CV is applied to the training set. It consists in randomly splitting the training data into  $K = 5$  folds. The model is trained using  $K - 1$  folds and validated on the remaining fold, outputting a score. The training is repeated until each fold is used as a validation set. The average of the recorded scores is the performance metric of the model. Finally, the entire training set is used to train each network with the previously selected set of hyperparameters. The results are outputted on the test set.

We use the Tree-Parzen algorithm (Bergstra et al., 2011) to select hyperparameters iteratively in an informed manner. We define a search space for each hyperparameter with specific distribution and boundary values. These values are described in Table 7. A set of hyperparameters is randomly sampled, and the model is scored on each of the five validation folds. These five validation scores are averaged, and a new set of hyperparameters is sampled based on the value of the average score. The sampling of hyperparameters sets is repeated 200 times.

For the application to the two patient data sets, we perform a double 5-fold CV on the entire dataset, because we have relatively small datasets and want to mimic an external test set. This strategy was first illustrated by Matsui et al. (2012). First, the real patient cohort is split into five folds: this is the outer loop. Then, we select one of the five folds as a test set and perform a 5-fold CV on the remaining data for each hyperparameter set: this is the inner loop. We choose the hyperparameters configuration with the minimum average validation loss obtained on the five folds of the inner loop. Finally, we fit the model with these optimal hyperparameters on the four folds of the outer loop and calculate predictions on the remaining test fold of the outer loop. This procedure is repeated on all the folds of the outer loop.

Regarding the IF, it has been shown that the performance of random forests is relatively insensitive to changes in their hyperparameter values (Probst et al., 2019). Therefore, the default hyperparameter values are used in the implementation of IF. The number of variable pairs to sample for each split equals  $\sqrt{p}/2$ . The number of trees constituting each forest is set to 2,000.

## 3.3 Data

The models are trained on 2 types of data: simulated data and real patient data sets. The synthetic data are generated to examine the operating characteristics and performances of the modeling techniques, while 2 high-dimensional patient clinical trial data sets are used for illustrative purposes.

### 3.3.1 Simulation study

In the first setting, we simulate nonlinear interactions between the biomarkers and the treatment variable using a full biomarker-by-treatment interaction model.

Rothwell (2005) put forward that the only reliable approach for assessing the predictiveness of biomarkers is to test their interaction with the treatment and introduce a full biomarker-by-treatment interaction model. We can simulate

data based on this model:

$$h(t|\tau, X) = h_0(t) \exp \left( \alpha_\tau \tau + \sum_{i=1}^p \beta_{i1} f_i(X_i) + \sum_{i=1}^p \beta_{i2} f_i(X_i) \tau \right). \quad (5)$$

In this model, we add non-linearity with the choice of the function  $f$ , which enables the building of complex interactions with the treatment. Our model extends the model from Haller et al. (2019) which considered the case of a single biomarker.

Here,  $\alpha_\tau$  is chosen as  $\alpha_\tau = \ln(0.75) \approx -0.288$ . We set  $\beta_{i1} = 0.288$ ,  $f_i(X) = (2X - 1)^2$  and  $\beta_{i2} = -0.9$ . The biomarkers are generated from a uniform distribution:  $X_i \sim \mathcal{U}_{[0,1]}$ . Since we intend to simulate an RCT, a total of  $n$  patients per data set are randomly assigned with a 1:1 ratio to the experimental or control arm, with  $P(\tau = \frac{1}{2}) = P(\tau = -\frac{1}{2}) = \frac{1}{2}$ .

Survival times are generated from a Weibull distribution. Thus, the risk can be written as follows:

$$h(t|\tau, X) = b^{-a} a t^{a-1} \exp \left( \alpha_\tau \tau + \sum_{i=1}^p \beta_{i1} f_i(X_i) + \sum_{i=1}^p \beta_{i2} f_i(X_i) \tau \right) \quad (6)$$

with  $a$  the shape parameter and  $b$  the scale parameter. For all scenarios, we generate exponential survival times (corresponding to a shape parameter  $a = 1$ ) with a time-constant baseline hazard rate. Using the inverse of the cumulative risk function for a Weibull distribution, we compute the theoretical survival probabilities (see details in Supplemental material):

$$S(t|X) = \exp \left( - \int_0^t h(s|X) ds \right) = \exp(-H_0(t) \exp(\beta X)) \quad (7)$$

A cohort of size  $n$  individuals ( $n \in \{2,000; 20,000\}$ ) is generated for each set, split into 50% for the training set and 50% for the test set. We generate independent censoring, and consider two censoring rates: a moderate censoring rate of 20% and a large censoring rate of 50%.  $q = 20$  variables are generated for each set. Among  $q$ , only  $p = 10$  biomarkers are really prognostic. For each scenario, 100 replications are performed.

In the second data generation process, nonlinear interactions are simulated based on a Friedman's random function generator (Friedman, 2001) in an accelerated failure time (AFT) model. Friedman's random function generator allows us to generate random functions with second-order interactions between the survival data and the explanatory variables and strong nonlinear effects. It is based on an AFT model, that assumes that the relationship between the logarithm of survival time  $T$  and the variables is linear. The random function generator is defined as:

$$\log T = m(X) + W \text{ with } W \sim \Gamma(2, 1).$$

A vector of variables  $X = (X_1, \dots, X_{20})$  is generated with  $X \sim \mathcal{N}(0, I)$ .  $m(X)$  is defined by Friedman's random function generator:

$$m(X) = \sum_{l=1}^{10} a_l g_l(R_l).$$

$\{a_l\}_1^{10}$  are randomly generated from a uniform distribution ( $a_l \sim \mathcal{U}_{[-1,1]}$ ).  $R_l$  is a random subset of the input vector  $X$  of size  $n_l = 5$ , implying high-order interaction effects. With Friedman's function generator, the input variables are associated with the survival time at different levels:

$$g_l(R_l) = \exp \left\{ -\frac{1}{2} (R_l - \mu_l)^T V_l (R_l - \mu_l) \right\}. \quad (8)$$

Each mean vector  $\{\mu_l\}_1^{10}$  is randomly generated with  $\mu_l \sim \mathcal{N}(0, 1)$ . The matrix of variance-covariance  $V_l$  is also randomly generated:  $V_l = U_l D_l U_l^T$  with  $U_l$  an orthonormal random matrix,  $D_l = \text{diag}\{d_{l,1}, \dots, d_{l,n_l}\}$  and  $\sqrt{d_{lk}} \sim \mathcal{U}(0.1, 2.0)$ . Finally, we obtain the survival times by applying the exponential:  $\exp(\log(T))$ . This is the AFT-Friedman method.

Henderson et al. (2020) adapt the flexible random function generator to the analysis of treatment effect by introducing a second generator interacting with the treatment variable. For this purpose, the AFT-Friedman model can be rewritten as:

$$\log T = m_1(X) + \tau \times m_2(X) + W \text{ with } W \sim \Gamma(2, 1), \quad (9)$$

where  $m_2(X)$  is defined as :

$$m_2(X) = \sum_{i=1}^{10} a_{2i} g_{2i}(R_{2i}).$$

The coefficients  $a_{2l}$  are randomly generated from a uniform distribution  $a_{2l} \sim \mathcal{U}_{[-0.2, 0.3]}$ . A total of  $n$  patients per data set were randomly assigned (1 : 1) to the experimental or control arm, with  $P(\tau = 1) = P(\tau = 0) = \frac{1}{2}$ .

By using the inverse of the cumulative risk function for a log-normal distribution, we are able to compute the theoretical survival probabilities (details in Supplemental material) :

$$S(t|X) = \exp \left( - \int_0^t h(s|X) ds \right) = \exp \left( - H_0(t \exp(m_1(X) + \tau \times m_2(X))) \right) \quad (10)$$

A cohort of size  $n$  individuals ( $n \in \{2,000; 20,000\}$ ) is generated for each set, split into 50% for the training set and 50% for the test set. We generate independent censoring, and considered a moderate censoring rate of 20%. For each scenario, 100 replications are performed.

### 3.4 Application on cancer data sets

We apply the methods to gene expression data from a meta-analysis of neoadjuvant trials that included 614 breast cancer patients treated by anthracyclines alone or anthracyclines plus taxanes (Ternès et al., 2018). We also use data from an RCT including 1,574 patients, which evaluates the effect of adjuvant trastuzumab in breast cancer (Pogue-Geile et al., 2013).

#### 3.4.1 Breast cancer study on taxane chemotherapy

We apply the models to a meta-analysis of neoadjuvant trials that included 614 breast cancer patients treated by anthracycline-based chemotherapy with ( $n = 507$ ) or without ( $n = 107$ ) taxane. The dataset is composed of  $p = 1,689$  genes. This cohort is available in the biospear(Ternès et al., 2018) R package that is publicly available.

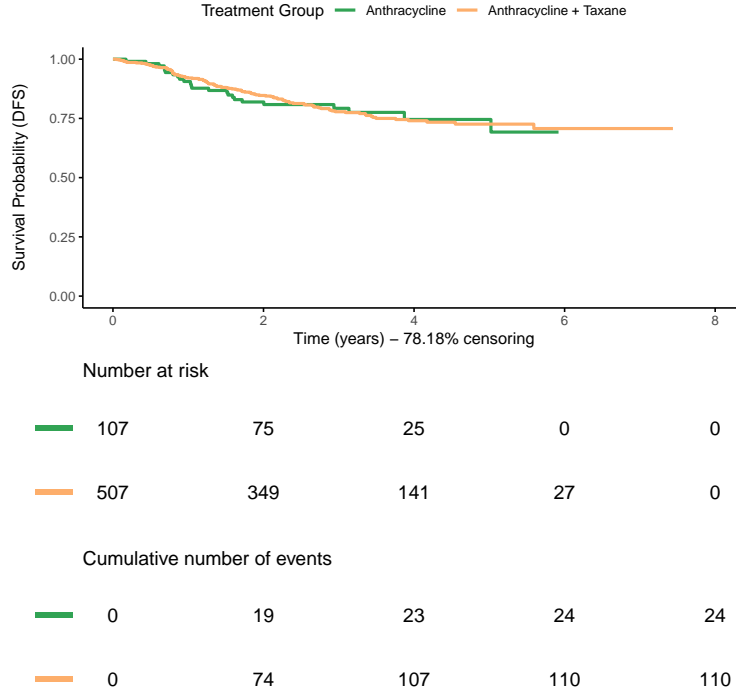


Figure 1: Kaplan-Meier curves for the breast cancer cohort on taxane chemotherapy.

#### 3.4.2 Breast cancer cohort with adjuvant trastuzumab

The models are also compared on data from an RCT funded by the National Cancer Institute and the National Institute of Health. This randomized phase III clinical trial evaluated the effect of adding trastuzumab to adjuvant chemotherapy

to disease-free survival in early breast cancer patients in Her2<sup>+</sup> breast cancer.

$n = 1,574$  patients were included in the trial:  $n = 795$  patients received chemotherapy, while  $n = 779$  others received chemotherapy and trastuzumab. For each patient, the expression of 462 genes is available in addition to standard clinicopathological variables such

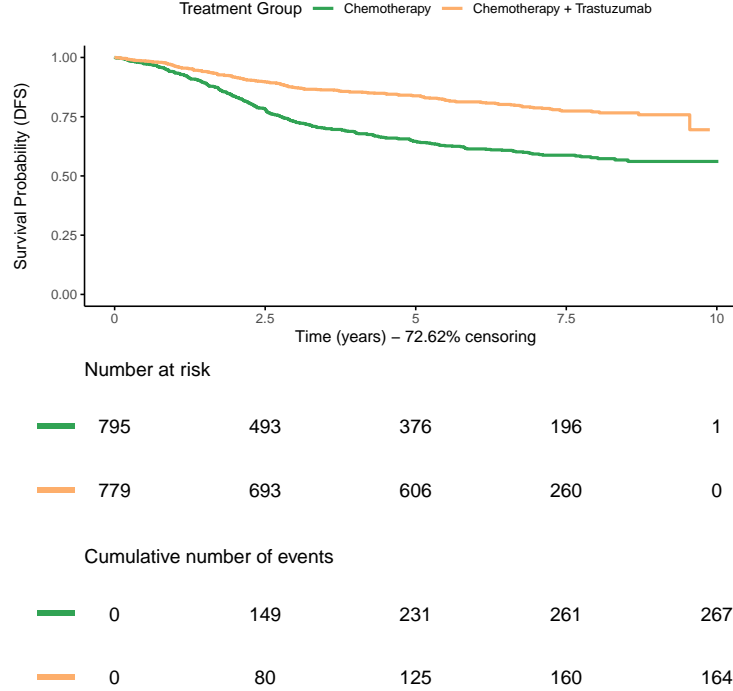


Figure 2: Kaplan-Meier curves for the breast cancer cohort with adjuvant trastuzumab.

### 3.5 Evaluation Measures

The treatment effect can be defined as the effect of treatment  $\tau$  on the outcome variable  $Y$ . Since  $Y$  is the observed outcome, we have:

$$Y = \begin{cases} Y(1) & \text{if } \tau = 1 \text{ (treatment)} \\ Y(0) & \text{if } \tau = 0 \text{ (control).} \end{cases}$$

When  $\tau = 1$ ,  $Y(0)$  is not observed: it is the counterfactual (Rubin, 1974).

In an RCT, assuming that  $Y(1)$  and  $Y(0)$  are independent from  $\tau|X$ , the treatment effect is defined as:

$$\mathbf{E}(Y(1) - Y(0)|X) = \mathbf{E}(Y|\tau = 1, X) - \mathbf{E}(Y|\tau = 0, X)$$

with  $X$  the characteristics of the patient.

The models are compared using metrics adapted to the evaluation of treatment benefit: the Concordance index for benefit ( $C_{\text{benefit}}$ ), the Integrated Calibration Index for benefit ( $ICI_{\text{benefit}}$ ), the E50 for benefit ( $E50_{\text{benefit}}$ ), and the root-mean-squared error (RMSE).

#### 3.5.1 Observed and predicted treatment benefit

We apply 2 matching procedures, either using variables or predicted benefit. First, we use a predicted score for each individual. The 2 groups of patients (control arm and treatment arm) are ranked based on the value of the predicted benefit. The data points are matched by aligning the sorted lists based on their ranks. Secondly, we apply a matching procedure based on patients' characteristics and the Mahalanobis distance. It is the distance between  $2n$  dimensional points scaled by the statistical variation in each component of the point.

The predicted benefit  $\hat{\theta}$  is defined as the difference between the individual survival probability at a given timepoint with the treatment option being tested minus the probability with the control for the same patient. Given that matching is not perfect, the predicted benefits are averaged for the pair of patients previously matched, and predicted benefit is defined as the average of the predicted benefits within each matched patient pair. We have :

$$\hat{\theta}_{u,v}(t) = \frac{[S_u(t|\tau = 1, X_u) - S_u(t|\tau = 0, X_u)]}{2} + \frac{[S_v(t|\tau = 1, X_v) - S_v(t|\tau = 0, X_v)]}{2}, \quad (11)$$

with  $u$  the patient in the treated arm ( $\tau = 1$ ), and  $v$  the patient in the control arm ( $\tau = 0$ ) for a given time  $t$ .

Observed treatment benefit  $\tilde{\theta}$  is defined as the difference in time-to-event for 2 matched patients. For each pair of patients ( $u$  belonging to the control arm, and  $v$  to the experimental arm), we calculate the observed treatment benefit using the following formula :

$$\tilde{\theta}_{u,v} = \mathbf{1}_{Statut_u} \times \mathbf{1}_{\tilde{T}_u < \tilde{T}_v} - \mathbf{1}_{Statut_v} \times \mathbf{1}_{\tilde{T}_v < \tilde{T}_u} \quad (12)$$

The first term of the equation  $\mathbf{1}_{Statut_u} \times \mathbf{1}_{\tilde{T}_u < \tilde{T}_v}$  equals 1 if the patient  $i$  has a shorter time-to-event compared to patient  $v$ , and 0 otherwise. The reasoning is the same for the second term of the equation (for patient  $v$ ). When the shortest survival time is censored, the treatment effect is not observed for the patient pair and equals 0.

Thus, for each pair of patients, the observed treatment benefit can take one of the following values: 1 for observed treatment benefit, 0 for no observed treatment effect, and  $-1$  for deleterious treatment effect.

### 3.5.2 Discrimination measures

The C-statistic at time  $t$  measures the discrimination ability of a model, indicating its ability to distinguish high-risk and low-risk patients for a fixed time horizon. Specifically, it estimates the probability of agreement, i.e., the probability that 2 patients randomly selected are ordered similarly in terms of survival prediction and in their observed survival data. Here, we use a concordance measure that accounts for the censored data using the inverse probability of censoring weighting (Uno et al., 2011). The concordance index for a horizon time  $t$  is then:

$$\hat{C}(t) = \frac{\sum_{i=1}^n \sum_{j=1}^n D_i \hat{G}(\tilde{T}_i)^{-2} \mathbb{I}\{\tilde{T}_i < \tilde{T}_j, \tilde{T}_i < t\} \mathbb{I}\{\hat{S}(t|X_i) < \hat{S}(t|X_j)\}}{\sum_{i=1}^n \sum_{j=1}^n D_i \hat{G}(\tilde{T}_i)^{-2} \mathbb{I}\{\tilde{T}_i < \tilde{T}_j, \tilde{T}_i < t\}} \quad (13)$$

The value of the C-statistic lies between 0 and 1, with 0.5 equivalent to a random prediction and 1 corresponding to a perfect ability to rank. We compute the C-statistic for all individuals.

C-for-benefit ( $C_{\text{benefit}}$ ) was introduced by Klavereen et al. (2017) as a measure of the discrimination capacity of the model. It is an extension of the C-statistic adapted to measure treatment benefit at a horizon time  $t$ . It represents the probability that, among 2 randomly chosen matched patient pairs, the pair with greater observed benefit also has a higher mean predicted benefit. It can be written as:

$$C_{\text{benefit}}(t) = P(\hat{\theta}_{p_k}(t) > \hat{\theta}_{p_l}(t) | \tilde{\theta}_{p_k}(t) > \tilde{\theta}_{p_l}(t)), \quad (14)$$

where  $p_k$  and  $p_l$  are 2 pairs of patients.

### 3.5.3 Calibration measures

To evaluate the calibration capacity of the model, we use measures based on the calibration curve. Calibration commonly refers to the agreement between predicted and observed probabilities for the outcome (Austin et al., 2020). Here, we are interested in the correspondence between the predicted and observed treatment effects.

Calibration can be assessed by a smoothed calibration curve obtained by a local regression of observed pairwise treatment effect on predicted pairwise treatment effect. The observed benefits are regressed on the predicted benefits using a locally weighted scatterplot smoother (loess). It is a non-parametric regression technique used to create a smoothing function through a scatterplot of data points. It combines multiple local regressions to fit a curve to subsets of the data, allowing it to capture complex patterns without assuming a specific global model.

The Integrated Calibration-for-Benefit ( $ICI_{\text{benefit}}$ ) (Rekkas et al., 2023; Maas et al., 2023) measures the average difference between predicted and smooth observed benefit across different levels of prediction determined by the empirical density function of the predicted pairwise treatment effect.  $E50_{\text{benefit}}$  represents the 50<sup>th</sup> percentile of the absolute distance



between predicted and smooth observed benefit. It assesses how well the predicted treatment effect matches the observed treatment effect at the median. It offers insight into the model’s calibration at the central point rather than across the entire prediction range. For these measures, null values indicate perfect calibration, meaning that the model’s predicted treatment benefits align perfectly with the observed benefits.

The calibration quantile plot (Bouvier et al., 2024) represents the average observed benefit versus predicted benefit in quantiles of predicted benefit. The predicted benefit is divided into 5 bins. In each bin, the average predicted benefit is compared to the observed benefit.

### 3.5.4 Root mean squared error

The predictive accuracy of the models is compared using the root mean squared error (RMSE)(Rekkas et al., 2023) adapted to time-to-event data. We compute RMSE for simulated data, where the true  $\theta$  is known. We then have :

$$\text{RMSE} = \sqrt{\frac{1}{n} \sum_{i=1}^n (\theta_i(t) - \hat{\theta}_i(t))^2}, \quad (15)$$

with  $\theta_i$  the true treatment benefit for individual  $i$  at time  $t$ .  $\hat{\theta}_i$  is the predicted benefit for individual  $i$ , that is, the difference in survival probabilities at a pre-specified time point  $t$  for one patient with and without treatment:

$$\hat{\theta}_i(t) = S_i(t|\tau = 1, X_i) - S_i(t|\tau = 0, X_i).$$

### 3.5.5 Bootstrap confidence intervals

Expected survival probabilities are estimated at specific time points (at  $t = 2$  and  $t = 5$  years), and bootstrap confidence intervals (CI) are constructed following the approach proposed by Roblin et al. (2024).

With this approach, the data is divided into a training set and a test set.  $M = 200$  bootstrap sets are sampled with replacement from the training set. The model is trained for each of these  $M$  subsets. It allows for the estimation of  $M$  survival probabilities at time  $t$  for a given patient  $i$  from the test set, noted as  $\hat{S}_i(t) = \{\hat{S}_{i(1)}(t), \dots, \hat{S}_{i(M)}(t)\}$ . The percentile method is then used to obtain confidence intervals at level  $1 - \theta$  for  $\hat{S}_i(t)$  based on the distribution of  $\hat{S}_{\text{all}}(t)$ :

$$\text{CI}_{1-\theta} = \left[ q_{\frac{\theta}{2}} \left( \hat{S}_i(t) \right), q_{1-\frac{\theta}{2}} \left( \hat{S}_i(t) \right) \right] \quad (16)$$

where  $q_{\frac{\theta}{2}}$  and  $q_{1-\frac{\theta}{2}}$  are percentiles computed using the empirical distribution of the  $M$  values. Here,  $\theta = 5\%$  and the  $2.5^{\text{th}}$  and  $97.5^{\text{th}}$  percentiles are computed using the empirical distribution of the  $M$  survival probabilities.

We calculate the CI for the survival probabilities of a patient  $i$  in the treatment arm ( $\hat{S}_{i,\text{trt}}(t)$ ) and the matched patient  $j$  in the control arm ( $\hat{S}_{j,\text{ctrl}}(t)$ ). The matching procedure is based on patients’ characteristics to ensure consistent matched pairs across all models.

## 4 Results

### 4.1 Results on the simulation sets

#### 4.1.1 Data generation process 1

The results reported here are the ones obtained using data simulated from the Weibull biomarker-by-treatment model with nonlinear interactions.

In Table 1, the highest average C-statistic and  $C_{\text{benefit}}$  were obtained with the IF model. It was also the closest to the oracle value. ALASSO obtained the lowest value in terms of  $C_{\text{benefit}}$ , which could indicate that the linear ALASSO model has difficulty capturing the treatment by biomarker interactions, whereas IF, due to its specific design for such interactions, demonstrates superior performance in modeling them.

$E50_{\text{benefit}}$  and  $ICI_{\text{benefit}}$  values remained substantially above zero across all models, which could highlight difficulties to obtain solid calibration or limitations of the matching procedure between control group patients and treatment group patients. In contrast, RMSE values approached zero, particularly for ALASSO.

If we only consider the machine learning methods, IF performed well in terms of discrimination performances and accuracy (higher concordance indices and lower RMSE), while FNNs had better calibration performances (lower

$E_{50_{\text{benefit}}}$  and  $ICI_{\text{benefit}}$ ). Of note, CoxCC and CoxTime had close results, which is as expected, as we did not simulate any interaction with time.

Table 1 also present the results of models trained on an expanded cohort of patients ( $n = 10,000$ ). The results remain largely consistent between  $n = 1,000$  and  $n = 10,000$ . For the machine learning methods, both the C-statistics and RMSE show only minor improvements compared to models trained on a smaller cohort. Meanwhile,  $C_{\text{benefit}}$  decreases slightly, whereas  $E_{50_{\text{benefit}}}$  and  $ICI_{\text{benefit}}$  exhibit slight increases.

Table 1: Average value at median time across the 100 simulation sets for data generation process 1.

Model	$n = 1,000$					$n = 10,000$				
	C	$C_{\text{benefit}}$	$E_{50_{\text{benefit}}}$	$ICI_{\text{benefit}}$	RMSE	C	$C_{\text{benefit}}$	$E_{50_{\text{benefit}}}$	$ICI_{\text{benefit}}$	RMSE
Oracle	0.613 ( $\pm 0.013$ )	0.562 ( $\pm 0.025$ )				0.615 ( $\pm 0.004$ )	0.557 ( $\pm 0.009$ )			
ALASSO	0.567 ( $\pm 0.014$ )	0.504 ( $\pm 0.028$ )	0.373 ( $\pm 0.062$ )	0.373 ( $\pm 0.059$ )	<b>0.118</b> ( $\pm 0.026$ )	0.568 ( $\pm 0.004$ )	0.499 ( $\pm 0.008$ )	<b>0.374</b> ( $\pm 0.021$ )	<b>0.376</b> ( $\pm 0.021$ )	<b>0.103</b> ( $\pm 0.006$ )
CoxCC	0.545 ( $\pm 0.018$ )	0.546 ( $\pm 0.043$ )	0.321 ( $\pm 0.117$ )	<b>0.321</b> ( $\pm 0.116$ )	0.212 ( $\pm 0.041$ )	0.581 ( $\pm 0.008$ )	<b>0.543</b> ( $\pm 0.021$ )	0.425 ( $\pm 0.0042$ )	0.42 ( $\pm 0.042$ )	0.171 ( $\pm 0.022$ )
CoxTime	0.543 ( $\pm 0.016$ )	0.541 ( $\pm 0.04$ )	<b>0.320</b> ( $\pm 0.107$ )	0.325 ( $\pm 0.015$ )	0.217 ( $\pm 0.045$ )	0.581 ( $\pm 0.006$ )	0.538 ( $\pm 0.02$ )	0.435 ( $\pm 0.036$ )	0.431 ( $\pm 0.037$ )	0.169 ( $\pm 0.019$ )
IF	<b>0.575</b> ( $\pm 0.015$ )	<b>0.561</b> ( $\pm 0.04$ )	0.468 ( $\pm 0.036$ )	0.452 ( $\pm 0.035$ )	0.195 ( $\pm 0.025$ )	<b>0.601</b> ( $\pm 0.004$ )	0.539 ( $\pm 0.011$ )	0.473 ( $\pm 0.015$ )	0.479 ( $\pm 0.013$ )	0.164 ( $\pm 0.008$ )

The value in brackets is the standard deviation across the 100 simulation sets. The highest C values and lowest  $E_{\text{benefit}}$ ,  $ICI_{\text{benefit}}$  and RMSE values are in bold. Patients are matched on predicted benefit. 50% censoring.

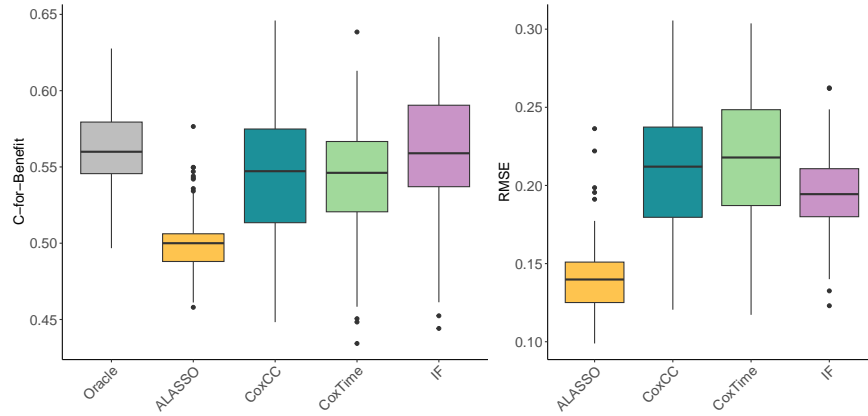


Figure 3:  $C_{\text{benefit}}$  and RMSE values for each model in data generation process 1. Each boxplot displays 100 points corresponding to each simulated set.

We also compared the models at different time points (Supplementary material Table 8), and for different levels of censoring (Supplementary material Table 9, Setting 1). All the results were improved when the censoring rate was lower (20% instead of 50%). Regarding the choice of the horizon time, the oracle values decreased over time, while the models performed similarly between the first and third quartiles of the time range.

The models were also compared using a matching procedure based on patient's characteristics (Table 9, Setting 2). All the models performed worse compared to using a matching procedure based on predicted treatment benefit. As noted by Klavaren et al. (2017), this is expected as the predicted treatment benefit for 2 patients within a pair matched by patient characteristics tends to be less similar.

#### 4.1.2 Data generation process 2

In Table 2, CoxCC, CoxTime, and IF exhibit comparable performances, with C values close to each other. CoxTime achieves the highest  $C_{\text{benefit}}$  at 0.616, with CoxCC and IF closely following. CoxTime also yields the lowest  $E_{50_{\text{benefit}}}$  and  $ICI_{\text{benefit}}$ , at 0.134 and 0.153. ALASSO consistently shows lower concordance values compared to the other models.

Table 2 also presents the the results for the model trained on a larger sample size. The results demonstrate only subtle differences across the evaluated metrics compared to the results obtained with a smaller sample size.

Table 2: Average value at median time across the 100 simulation sets for data generation process 2.

Model	$n = 1,000$					$n = 10,000$				
	C	$C_{\text{benefit}}$	$E50_{\text{benefit}}$	$ICI_{\text{benefit}}$	RMSE	C	$C_{\text{benefit}}$	$E50_{\text{benefit}}$	$ICI_{\text{benefit}}$	RMSE
Oracle	0.841 ( $\pm 0.038$ )	0.583 ( $\pm 0.047$ )				0.838 ( $\pm 0.039$ )	0.584 ( $\pm 0.039$ )			
ALASSO	0.734 ( $\pm 0.093$ )	0.583 ( $\pm 0.047$ )	0.328 ( $\pm 0.146$ )	0.332 ( $\pm 0.136$ )	0.094 ( $\pm 0.035$ )	0.719 ( $\pm 0.077$ )	0.583 ( $\pm 0.035$ )	0.326 ( $\pm 0.144$ )	0.337 ( $\pm 0.129$ )	0.091 ( $\pm 0.030$ )
CoxCC	<b>0.876</b> ( $\pm 0.048$ )	0.611 ( $\pm 0.041$ )	0.143 ( $\pm 0.071$ )	0.164 ( $\pm 0.058$ )	0.086 ( $\pm 0.019$ )	<b>0.897</b> ( $\pm 0.046$ )	<b>0.599</b> ( $\pm 0.039$ )	0.148 ( $\pm 0.070$ )	0.168 ( $\pm 0.064$ )	0.064 ( $\pm 0.012$ )
CoxTime	0.868 ( $\pm 0.057$ )	<b>0.616</b> ( $\pm 0.042$ )	<b>0.134</b> ( $\pm 0.061$ )	<b>0.153</b> ( $\pm 0.053$ )	0.091 ( $\pm 0.021$ )	0.896 ( $\pm 0.048$ )	0.598 ( $\pm 0.036$ )	<b>0.136</b> ( $\pm 0.068$ )	<b>0.153</b> ( $\pm 0.060$ )	<b>0.061</b> ( $\pm 0.012$ )
IF	0.875 ( $\pm 0.051$ )	0.608 ( $\pm 0.037$ )	0.146 ( $\pm 0.090$ )	0.172 ( $\pm 0.079$ )	<b>0.081</b> ( $\pm 0.021$ )	0.856 ( $\pm 0.051$ )	0.577 ( $\pm 0.042$ )	0.159 ( $\pm 0.116$ )	0.185 ( $\pm 0.111$ )	0.085 ( $\pm 0.023$ )

The value in brackets is the standard deviation across the 100 simulation sets. The highest C values and lowest  $E_{\text{benefit}}$  and RMSE values are in bold. Patients are matched on predicted benefit. 50% censoring.

## 4.2 Results on the two breast cancer data sets

FNN-based methods, IF and ALASSO were applied on 2 breast cancer clinical trial data sets. All comparison measures were computed on the test set at 2 and 5 years. These times were chosen as these are usual times of interest for clinical investigators for early breast cancer.

### 4.2.1 Individualized treatment effects of taxane chemotherapy

The results are presented in Table 3. The machine learning models achieved reasonable performances: CoxCC obtained the highest  $C_{\text{benefit}}$  and the lowest  $ICI_{\text{benefit}}$ , and IF the lowest  $E50_{\text{benefit}}$ . The adaptive CoxPH method obtained lower performances on the treatment benefit measures. In this data set, the machine learning methods seem better able to capture the biomarker-by-treatment interactions in the data, which could highlight the existence of high-order interactions and nonlinear effects.

Table 3: Measures at 2 and 5 years for the meta-analysis the effect of taxane chemotherapy. - Matching on predicted benefit.

Model	$t = 2$				$t = 5$			
	C	$C_{\text{benefit}}$	$E50_{\text{benefit}}$	$ICI_{\text{benefit}}$	C	$C_{\text{benefit}}$	$E50_{\text{benefit}}$	$ICI_{\text{benefit}}$
ALASSO	<b>0.733</b>	0.605	0.266	0.267	<b>0.703</b>	<b>0.603</b>	0.240	0.203
CoxCC	0.658	<b>0.619</b>	0.07	<b>0.076</b>	0.550	0.599	<b>0.069</b>	<b>0.094</b>
CoxTime	0.689	0.609	0.086	0.103	0.550	0.579	0.094	0.100
IF	0.694	0.587	<b>0.032</b>	0.108	0.549	0.571	0.099	0.339

The highest C values and lowest  $E_{\text{benefit}}$ ,  $ICI_{\text{benefit}}$  and RMSE values are in bold.

Two matched patients were sampled from the dataset. Patient 1 is part of the control group, with a survival time of 1.5 years without censoring. Patient 2 is part of the treatment group, followed for 2.5 years before being lost to follow-up. Among the models, ALASSO demonstrates the narrowest CIs, indicating higher precision in its predictions, mimicking a bit the low RMSE from the simulation study, but without having the best c-for-benefit or calibration measures. Across all models, Patient 2 consistently shows a higher predicted mean survival probability than Patient 1, with narrower CI. For example, with the CoxTime model, Patient 1 has a mean survival probability of 0.820 and a CI of [0.558, 0.953], whereas Patient 2 has a mean survival probability of 0.942 with a CI of [0.858, 0.953]. Figure 4 illustrates the distribution of predicted survival probabilities, showing a wider spread for Patient 1 compared to Patient 2.

Table 4: Mean expected survival probabilities and associated CI at 2 years for 2 patients from the breast cancer cohort on taxane chemotherapy.

Patient	ALASSO	CoxCC	CoxTime	IF
Patient 1 with control	0.846 [0.845, 0.848]	0.857 [0.668, 0.968]	0.820 [0.558, 0.953]	0.772 [0.767, 0.778]
Patient 2 with treatment	0.894 [0.892, 0.895]	0.939 [0.829, 0.989]	0.942 [0.858, 0.983]	0.928 [0.925, 0.931]

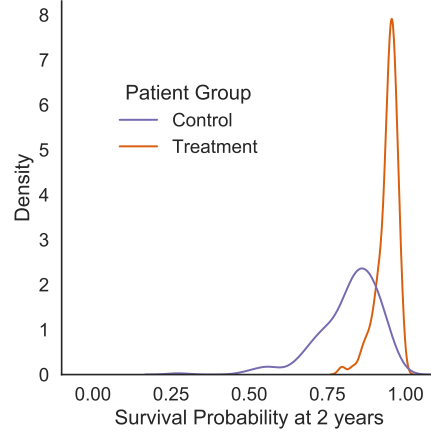


Figure 4: Density estimate of expected survival probabilities at 2 years computed with CoxTime for two patients with breast cancer.

#### 4.2.2 Individualized treatment effects of adjuvant trastuzumab

For the second breast cancer data set, we observed in Table 5 that ALASSO obtained the highest  $C_{\text{benefit}}$ . This could suggest that there are limited nonlinear and high-order interactions with the treatment in the data set, and that the more flexible machine learning method don't capture a stronger signal. On average, ALASSO selected 22 biomarker main effects and 16 biomarker-by-treatment interactions.

In terms of calibration, the machine-learning-based methods obtained better results compared to ALASSO, with lower values in terms of  $ICI_{\text{benefit}}$  and  $E50_{\text{benefit}}$ .

Table 5: Measures at 2 and 5 years in the RCT on adjuvant trastuzumab. - Matching on predicted benefit.

Model	$t = 2$				$t = 5$			
	C	$C_{\text{benefit}}$	$E50_{\text{benefit}}$	$ICI_{\text{benefit}}$	C	$C_{\text{benefit}}$	$E50_{\text{benefit}}$	$ICI_{\text{benefit}}$
ALASSO	<b>0.677</b>	<b>0.641</b>	0.231	0.220	<b>0.692</b>	<b>0.659</b>	0.170	0.139
CoxCC	0.590	0.507	<b>0.039</b>	<b>0.049</b>	0.584	0.516	0.053	0.052
CoxTime	0.582	0.505	0.087	0.093	0.584	0.523	<b>0.037</b>	<b>0.046</b>
IF	0.624	0.571	0.069	0.077	0.618	0.521	0.069	0.084

The highest C values and lowest  $E_{\text{benefit}}$ ,  $ICI_{\text{benefit}}$  and RMSE values are in bold.

In Table 6, we further studied the point estimates of expected survival. Patient 3 has a survival time of 8 years and 1 month, with censored follow-up, and received chemotherapy. Patient 4 has a survival time of 8 years and 6 months, also with censored follow-up, and received both chemotherapy and trastuzumab. The mean survival probability for all patients is high at 2 years, aligning with the observed survival times of these two patients. The CI are wider for Patient 3 under the control condition. For example, with the CoxCC model, the mean survival probability at 2 years for Patient 3 was 0.822 with a confidence interval of  $[0.64, 0.932]$ , compared to 0.939 for Patient 2, with a narrower CI of  $[0.862, 0.974]$ .

## 5 Discussion

In this paper, we compared 2 FNNs methods adapted to survival (CoxCC and CoxTime) and one random forests model (IF) for their ability to predict treatment benefit in the context of time-to-event data, using a linear CoxPH model with an adaptive LASSO penalty as a benchmark method. The comparison was conducted on 2 simulation sets: one introducing nonlinear interaction with treatment and another based on Friedman's random function generator with non-linear and two-order interactions. Additionally, the models were tested on 2 breast cancer data sets.

The machine learning methods performed well in data generation process 1, especially in terms of discrimination capabilities for IF and calibration for FNNs. For data generation process 2, the performances of the machine learning methods are slightly higher than the reference value in terms of discrimination.

Table 6: Mean expected survival probabilities and associated CI at 2 years for 2 patients from the breast cancer cohort on adjuvant trastuzumab.

Patient	ALASSO	CoxCC	CoxTime	IF
Patient 3 with control	0.825 [0.823,0.826]	0.822 [0.64,0.932]	0.824 [0.702,0.912]	0.765 [0.760,0.77]
Patient 4 with treatment	0.951 [0.950,0.951]	0.939 [0.862,0.974]	0.921 [0.863,0.956]	0.918 [0.916,0.920]

With the first breast cancer data set evaluating the effect of taxane chemotherapy, the machine learning models achieved better prediction results compared to the CoxPH model with an adaptive LASSO penalty, suggesting that the data set has some complex biomarkers-by-treatment interactions. In the second data sets the adaptive lasso model had the best discrimination but the FNN or IF better calibration.

In this paper we used measures specifically adapted to treatment benefit evaluation in the context of time-to-event data. The assessment of treatment benefit prediction models has been an active area of research. Efthimiou et al. (2022) worked on developing measures of discrimination and calibration, extending the work of Klaveren et al. (2017) who introduced the C-for-benefit metric specifically for treatment benefit evaluation. We adapted their approach to time-to-event data by calculating this measure using survival probabilities. Additionally, we modified the RMSE metric to assess treatment benefit for time-to-event data by evaluating the difference between predicted and true treatment benefits, both derived from survival probabilities. Using adapted measures for treatment benefit is of crucial importance, as the standard concordance index was not able to capture the treatment benefit directly. Future work could include associating uncertainty measures with individualized treatment recommendations that could also take model uncertainty into account, for example using ensemble methods.

Our work is centered on the RCT framework, allowing the determination of causal relationships between an intervention and its outcome. However, the methods used in this paper could be adapted beyond RCTs and applied to real-world data cohorts by incorporating propensity scores or other causal approaches. Cui et al. (2023) proposed such an approach using causal forests, a machine learning method used to estimate heterogeneous treatment effects in observational studies.

Further work could focus on the relative contribution of the input variables, as it could enable us to identify specific biomarkers interacting with the treatment, and we could determine the biomarker-treatment score for patients defined as the cross-product between the coefficient of the interactions retained in the training set and their biomarkers. Determining the relative importance of the different input variables is challenging in the case of FNNs. As it is a nonlinear type of model, simply looking at the resulting weights and biases outputted by the model is not possible. Also, FNNs do not have an assumption of non-colinearity of the inputs. There could be informative interactions among groups of variables. To overcome this issue, different methodologies have been defined to assess variable contributions in FNNs that focus on the weights of the model (Garson, 1991) which could be explored. For the IF, we could evaluate the the Effect Importance Measure.

## 6 Acknowledgements

The authors acknowledge the National Surgical Adjuvant Breast and Bowel Project (NSABP) investigators of the B-31 trial who submitted data from the original study to dbGaP (dbGaP Study Accession: phs000826.v1.p1) and the NIH data repository. The B-31 trial was supported by: National Cancer Institute, Department of Health and Human Services, Public Health Service, Grants U10-CA-12027, U10-CA-69651, U10-CA-37377, and U10-CA-69974, and by a grant from the Pennsylvania Department of Health.

## 7 Declaration of conflicting interests

The authors declare no potential conflict of interests.

## References

L.R. Yates, J. Seoane, C. Le Tourneau, L.L. Siu, R. Marais, S. Michiels, J.C. Soria, P. Campbell, N. Normanno, A. Scarpa, J.S. Reis-Filho, J. Rodon, C. Swanton, and F. Andre. The european society for medical oncology (esmo) precision medicine glossary. *Annals of Oncology*, 29(1):30–35, 2018. ISSN 0923-7534. doi:10.1093/annonc/mdx707.

- D.B. Rubin. Estimating causal effects of treatments in randomized and nonrandomized studies. *Journal of Educational Psychology*, 66:688–701, 1974.
- H. Kvamme, O. Borgan, and I. Scheel. Time-to-event prediction with neural networks and cox regression. *Journal of Machine Learning Research*, 20(129):1–30, 2019.
- D. R. Cox. Regression Models and Life-Tables. *Journal of the Royal Statistical Society. Series B (Methodological)*, 34(2):187–220, 1972. ISSN 0035-9246.
- N. Ternès, F. Rotolo, G. Heinze, and S. Michiels. Identification of biomarker-by-treatment interactions in randomized clinical trials with survival outcomes and high-dimensional spaces. *Biometrical Journal*, 59:685–701, 7 2017. ISSN 15214036. doi:10.1002/bimj.201500234.
- J. Katzman, U. Shaham, J. Bates, A. Cloninger, T. Jiang, and Y. Kluger. Deepsurv: personalized treatment recommender system using a cox proportional hazards deep neural network. *BMC Medical Research Methodology*, 18, 2018. doi:10.1186/s12874-018-0482-1.
- D. Klaveren, E. Steyerberg, P. Serruys, and D. Kent. The proposed ‘concordance-statistic for benefit’ provided a useful metric when modeling heterogeneous treatment effects. *Journal of Clinical Epidemiology*, 94, 11 2017. doi:10.1016/j.jclinepi.2017.10.021.
- C.C.H.M. Maas, D. M. Kent, M.C. Hughe, R. Dekker, H. F. Lingsma, and D. van Klaveren. Performance metrics for models designed to predict treatment effect. *BMC Medical Research Methodology*, 23, 12 2023. ISSN 14712288. doi:10.1186/s12874-023-01974-w.
- A. Rekkas, P.R. Rijnbeek, D. M. Kent, E.W. Steyerberg, and D. van Klaveren. Estimating individualized treatment effects from randomized controlled trials: a simulation study to compare risk-based approaches. *BMC Medical Research Methodology*, 23, 12 2023. ISSN 14712288. doi:10.1186/s12874-023-01889-6.
- F. Bouvier, A. Chaimani, E. Peyrot, F. Gueyffier, G. Grenet, and R. Porcher. Estimating individualized treatment effects using an individual participant data meta-analysis. *BMC Medical Research Methodology*, 24, 12 2024. ISSN 14712288. doi:10.1186/s12874-024-02202-9.
- R. Tibshirani. Regression Shrinkage and Selection via the Lasso. *Journal of the Royal Statistical Society. Series B (Methodological)*, 58(1):267–288, 1996. ISSN 0035-9246.
- R. Tibshirani. The Lasso Method for Variable Selection in the Cox Model. *Statistics in Medicine*, 16(4):385–395, 1997. ISSN 1097-0258. doi:10.1002/(SICI)1097-0258(19970228)16:4<385::AID-SIM380>3.0.CO;2-3.
- J. Fan and J. Lv. Sure independence screening for ultrahigh dimensional feature space. *Journal of the Royal Statistical Society. Series B: Statistical Methodology*, 70:849–911, 11 2008. ISSN 13697412. doi:10.1111/j.1467-9868.2008.00674.x.
- R. Hornung and A.-L. Boulesteix. Interaction forests: Identifying and exploiting interpretable quantitative and qualitative interaction effects. *Computational Statistics & Data Analysis*, 171:107460, 2022. ISSN 0167-9473. doi:10.1016/j.csda.2022.107460.
- R Peto. Statistical aspects of cancer trials. *Treatment of cancer*, pages 867–871, 1982.
- J. Bergstra, R. Bardenet, Y. Bengio, and B. Kégl. Algorithms for hyper-parameter optimization. In J. Shawe-Taylor, R. Zemel, P. Bartlett, F. Pereira, and K.Q. Weinberger, editors, *Advances in Neural Information Processing Systems*, volume 24, pages 2546–2554. Curran Associates, Inc., 2011.
- Shigeyuki Matsui, Richard Simon, Pingping Qu, John D. Shaughnessy, Bart Barlogie, and John Crowley. Developing and validating continuous genomic signatures in randomized clinical trials for predictive medicine. *Clinical Cancer Research*, 18:6065–6073, 11 2012. ISSN 15573265. doi:10.1158/1078-0432.CCR-12-1206.
- P. Probst, A.-L. Boulesteix, and B. Bischl. Tunability: Importance of hyperparameters of machine learning algorithms. *The Journal of Machine Learning Research*, 20(1):1934–1965, 2019.
- P. M. Rothwell. Treating individuals 2: Subgroup analysis in randomised controlled trials: Importance, indications, and interpretation. *Lancet*, 365:176–186, 1 2005. ISSN 01406736. doi:10.1016/S0140-6736(05)17709-5.
- B. Haller, K. Ulm, and A. Hapfelmeier. A simulation Study Comparing Different Statistical Approaches for the Identification of Predictive Biomarkers. *Computational and Mathematical Methods in Medicine*, 2019, 2019.
- Jerome H. Friedman. Greedy function approximation: A gradient boosting machine. *Annals of Statistics*, 29:1189–1232, 2001. ISSN 00905364. doi:10.2307/2699986.
- N.C. Henderson, T.L. Louis, G.L. Rosner, and R. Varadhan. Individualized treatment effects with censored data via fully nonparametric bayesian accelerated failure time models. *Biostatistics*, 21:50–68, 2020. ISSN 14684357. doi:10.1093/biostatistics/kxy028.

- N. Ternès, F. Rotolo, and S. Michiels. Biospear: An r package for biomarker selection in penalized cox regression. *Bioinformatics*, 34:112–113, 1 2018. ISSN 14602059. doi:10.1093/bioinformatics/btx560.
- Katherine L. Pogue-Geile, Chungyeul Kim, Jong Hyeon Jeong, Noriko Tanaka, Hanna Bandos, Patrick G. Gavin, Debora Fumagalli, Lynn C. Goldstein, Nour Sneige, Eike Burandt, Yusuke Taniyama, Olga L. Bohn, Ahwon Lee, Seung Il Kim, Megan L. Reilly, Matthew Y. Remillard, Nicole L. Blackmon, Seong Rim Kim, Zachary D. Horne, Priya Rastogi, Louis Fehrenbacher, Edward H. Romond, Sandra M. Swain, Eleftherios P. Mamounas, D. Lawrence Wickerham, Charles E. Geyer, Joseph P. Costantino, Norman Wolmark, and Soonmyung Paik. Predicting degree of benefit from adjuvant trastuzumab in nsabp trial b-31. *Journal of the National Cancer Institute*, 105:1782–1788, 12 2013. ISSN 00278874. doi:10.1093/jnci/djt321.
- H. Uno, T. Cai, M. J. Pencina, R. B. D’Agostino, and L. J. Wei. On the C-statistics for evaluating overall adequacy of risk prediction procedures with censored survival data. *Statistics in Medicine*, 30:1105–1117, 5 2011. ISSN 02776715. doi:10.1002/sim.4154.
- P. C. Austin, F. E. Harrell, and D. van Klaveren. Graphical calibration curves and the integrated calibration index (ici) for survival models. *Statistics in Medicine*, 39:2714–2742, 9 2020. ISSN 10970258. doi:10.1002/sim.8570.
- E. Roblin, P.H. Cournède, and S. Michiels. Confidence intervals of survival predictions with neural networks trained on molecular data. *Informatics in Medicine Unlocked*, 44:101426, 2024. ISSN 23529148. doi:10.1016/j.imu.2023.101426.
- O. Efthimiou, J. Hoogland, T.P.A. Debray, M. Seo, T. A. Furukawa, M. Egger, and I. R. White. Measuring the performance of prediction models to personalize treatment choice. *Statistics in Medicine*, 2022. doi:10.1002/sim.9665.
- Y Cui, M.R. Kosorok, E. Sverdrup, S. Wager, and R. Zhu. Estimating heterogeneous treatment effects with right-censored data via causal survival forests. *Journal of the Royal Statistical Society. Series B: Statistical Methodology*, 85:179–211, 4 2023. ISSN 14679868. doi:10.1093/jrsssb/qqac001.
- G. David Garson. Interpreting neural-network connection weights. *AI Expert*, 6(4):46–51, 1991. ISSN 0888-3785.
- R. Bender, Augustin. T., and M. Blettner. Generating survival times to simulate cox proportional hazards models. *Statistics in Medicine*, 24:1713–1723, 6 2005. ISSN 02776715. doi:10.1002/sim.2059.
- L. M. Leemis, L.-H. Shih, and K. Reynertson. Variate generation for accelerated life and proportional hazards models with time dependent covariates. *Statistics & Probability Letters*, 10(4):335–339, sep 1990. ISSN 01677152. doi:10.1016/0167-7152(90)90052-9.

## Supplementary Material

### A Hyperparameter search

Table 7: Hyperparameters search using Tree-Parzen Algorithm with the python package optuna.

Hyperparameter	Value
Activation function	{elu, relu, tanh}
Batch size	{8, 16, 32, 64, 128, 256}
Dropout rate	[0.01, 0.5]
$L_2$ regularization	[0.001, 0.1]
Learning rate	[0.001, 0.01]
Number of hidden layers	{1, 2, 3, 4}
Number of neurons per layer	[4, 128]
Optimization algorithm	{Adam, AdamAMSGRAD, RMSProp, SGDWR}

### B Simulated data

#### B.1 Details of computation

##### B.1.1 Data generation process 1

In this section, we introduce the calculation to obtain the theoretical survival values from the oracle model in the simulation data generation process 1.

To simulate survival times from a Weibull distribution, the following relationship can be used (Bender et al., 2005):

$$T = H_0^{-1}[-\log(1 - U)] \exp(\beta(X))$$

with  $U \sim \mathcal{U}[0, 1]$ . In the case of a Weibull risk function,  $\lambda > 0$  is the scale parameter,  $\kappa$  is the shape parameter, and the cumulative risk function is written as:

$$H_0(t) = \left(\frac{t}{\lambda}\right)^\kappa$$

The inverse of  $H_0$  is then written:

$$H_0^{-1}(u) = \lambda u^{1/\kappa}$$

We obtain:

$$T = \lambda[-\log(1 - U)]^{1/\kappa} \exp(\beta X)$$

The basis risk function  $h_0(t)$  is known and follows a certain probability distribution. In this case, we use the Weibull distribution. The risk function is then written as:

$$h(t|X) = \frac{\kappa}{\lambda} \left(\frac{t}{\lambda}\right)^{\kappa-1} \exp(\beta X)$$

with  $h_0(t) = \frac{\kappa}{\lambda} \left(\frac{t}{\lambda}\right)^{\kappa-1}$  the risk at baseline and  $\beta$  the coefficients vector. We then obtain the survival function from the instantaneous risk :

$$\begin{aligned} S(t|X) &= \exp\left(-\int_0^t h(s|X) ds\right) \\ &= \exp(-H_0(t) \exp(\beta X)). \end{aligned}$$



### B.1.2 Data generation process 2

In this section, we introduce the calculation to obtain the theoretical survival values from the oracle model in the simulation data generation process 2.

To simulate survival times from an AFT model and a random generator based on Friedman's function, the following relationship can be used (Leemis et al., 1990):

$$T = \frac{H_0^{-1}[-\log(1 - U)]}{\exp(m_1(X) + \tau \times m_2(X))},$$

with  $U \sim \mathcal{U}[0, 1]$ . In the case of a lognormal risk function, the cumulative risk function is written as :

$$H_0(t) = -\log \left[ 1 - \phi \left( \frac{\log(t) - \mu}{\sigma} \right) \right].$$

The inverse of  $H_0$  is then written:

$$H_0^{-1}(u) = \exp(\sigma \phi^{-1}(1 - \exp(-u)) + \mu).$$

We obtain:

$$T = \frac{1}{\exp(m_1(X) + \tau \times m_2(X))} \exp(\sigma \phi^{-1}(U) + \mu).$$

The basis risk function  $h_0(t)$  is known and follows a certain probability distribution. In this case, we use the log-normal distribution. The risk function is then written as:

$$h(t|X) = \exp(m_1(X) + \tau \times m_2(X)) h_0(t \exp(m_1(X) + \tau \times m_2(X))),$$

with  $h_0(t)$  the risk at baseline and  $\beta$  the coefficients vector. We then obtain the survival function from the instantaneous risk :

$$\begin{aligned} S(t|X) &= \exp\left(-\int_0^t h(s|X) ds\right) \\ &= \exp(-H_0(t \exp(m_1(X) + \tau \times m_2(X)))). \end{aligned}$$

## B.2 Kaplan Meier Curves for data generation process 1 and 2

We can see the Kaplan-Meier curves of the treatment group and the control group for one of the dataset in data generation process 1 and 2 in the following figures.

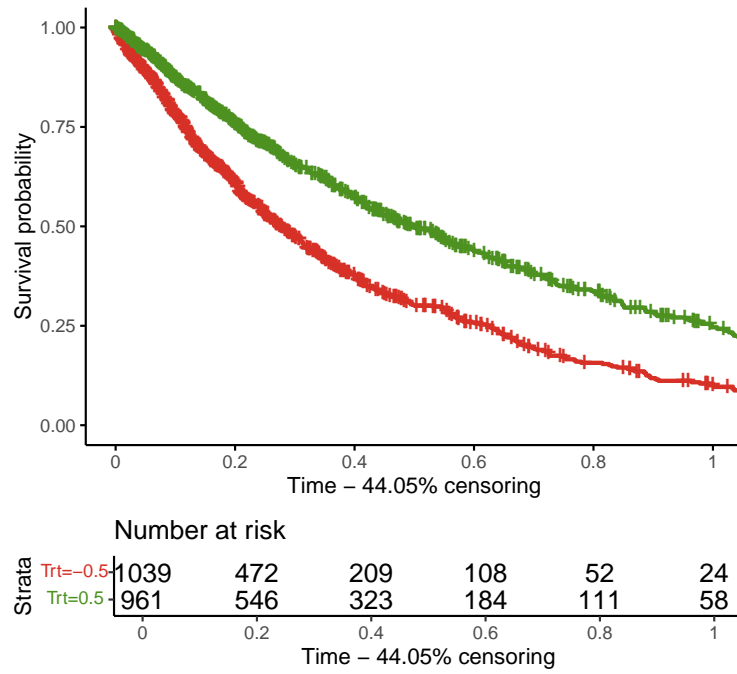


Figure 5: Kaplan-Meier curve for one simulation set in data generation process 1, with  $n = 20000$ .

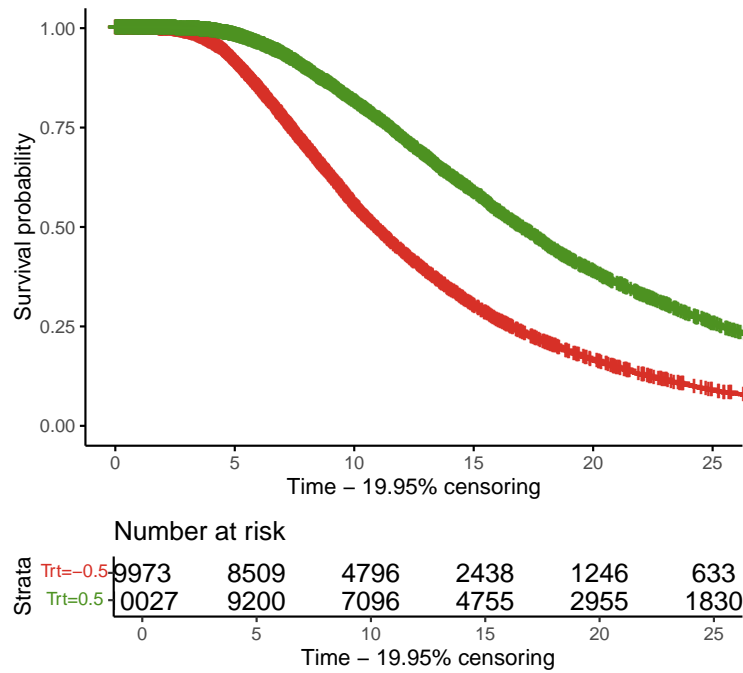


Figure 6: Kaplan-Meier curve for one simulation set in data generation process 2, with  $n = 20000$ .

### B.3 Detailed results for data generation process 1

Table 8: Average value at the first and third quartiles of time across the 100 simulation sets for data generation process 1.

Model	Q1					Q3				
	C	C <sub>benefit</sub>	E50 <sub>benefit</sub>	ICI <sub>benefit</sub>	RMSE	C	C <sub>benefit</sub>	E50 <sub>benefit</sub>	ICI <sub>benefit</sub>	RMSE
Oracle	0.619 (±0.021)	0.604 (±0.022)				0.613 (±0.013)	0.504 (±0.024)			
ALASSO	<b>0.571</b> (±0.019)	0.501 (±0.021)	0.515 (±0.033)	0.515 (±0.030)	<b>0.259</b> (±0.020)	0.569 (±0.013)	0.503 (±0.020)	0.440 (±0.044)	0.439 (±0.042)	<b>0.095</b> (±0.013)
CoxCC	0.543 (±0.017)	0.536 (±0.045)	0.395 (±0.137)	0.394 (±0.134)	0.309 (±0.029)	0.543 (±0.017)	<b>0.538</b> (±0.039)	0.338 (±0.114)	0.342 (±0.112)	0.118 (±0.026)
CoxTime	0.543 (±0.016)	0.537 (±0.039)	<b>0.388</b> (±0.113)	<b>0.388</b> (±0.127)	0.312 (±0.033)	0.543 (±0.016)	0.534 (±0.046)	<b>0.336</b> (±0.111)	<b>0.339</b> (±0.110)	0.124 (±0.029)
IF	<b>0.571</b> (±0.016)	<b>0.590</b> (±0.043)	0.499 (±0.051)	0.471 (±0.057)	0.307 (±0.018)	<b>0.575</b> (±0.013)	0.541 (±0.040)	0.479 (±0.036)	0.466 (±0.031)	0.099 (±0.014)

The value in brackets is the standard deviation across the 100 simulation sets. The highest C values and lowest E for benefit and RMSE values are highlighted in bold. Patients are matched on predicted benefit. There is 50% censoring.

Table 9: Average value at median time across the 100 simulation sets for data generation process 1.

Model	Setting 1					Setting 2				
	C	C <sub>benefit</sub>	E50 <sub>benefit</sub>	ICI <sub>benefit</sub>	RMSE	C	C <sub>benefit</sub>	E50 <sub>benefit</sub>	ICI <sub>benefit</sub>	RMSE
Oracle	0.615 (±0.013)	0.619 (±0.028)					0.559 (±0.028)			
ALASSO	0.569 (±0.013)	0.501 (±0.032)	0.684 (±0.035)	0.682 (±0.034)	<b>0.144</b> (±0.020)	0.503 (±0.02)	0.503 (±0.02)	0.442 (±0.042)	0.443 (±0.04)	<b>0.141</b> (±0.025)
CoxCC	0.550 (±0.017)	0.568 (±0.046)	<b>0.475</b> (±0.155)	<b>0.477</b> (±0.148)	0.212 (±0.037)	0.528 (±0.036)	<b>0.350</b> (±0.0099)	<b>0.349</b> (±0.01)	0.214 (±0.041)	0.219 (±0.041)
CoxTime	0.551 (±0.019)	<b>0.575</b> (±0.045)	0.483 (±0.151)	0.484 (±0.143)	0.206 (±0.038)	0.531 (±0.034)	0.360 (±0.084)	0.357 (±0.084)	0.357 (±0.084)	0.219 (±0.046)
IF	<b>0.590</b> (±0.013)	0.562 (±0.053)	0.694 (±0.027)	0.679 (±0.027)	0.173 (±0.023)	<b>0.539</b> (±0.036)	0.479 (±0.032)	0.488 (±0.037)	0.488 (±0.037)	0.195 (±0.025)

The value in brackets is the standard deviation across the 100 simulation sets. The highest C values and lowest E for benefit and RMSE values are highlighted in bold. Patients are matched on predicted benefit.

Setting 1: Matching on predicted benefit. There is 20% censoring.

Setting 2: Matching on covariates. There is 50% censoring.

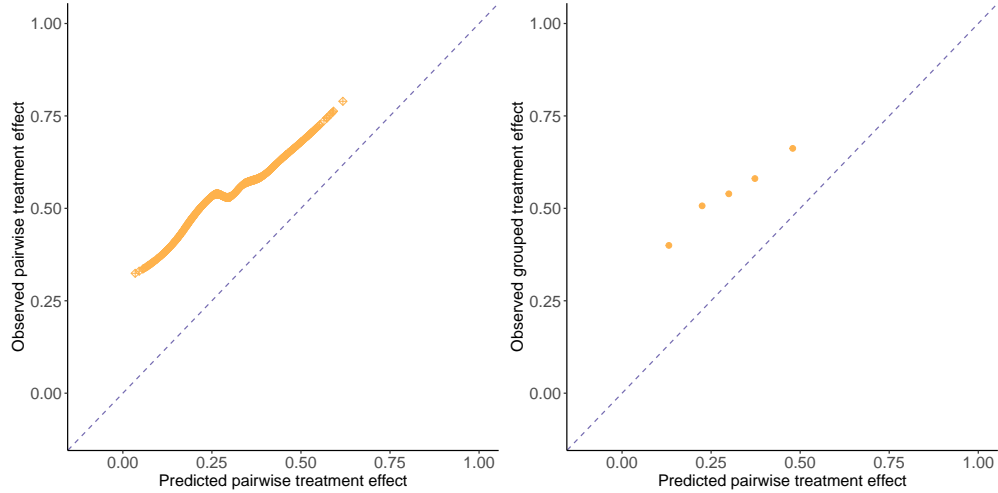


Figure 7: Calibration plot for one dataset in data generation process 1 and with CoxTime predictions. The left figure displays all the points, and the right figure shows quintiles.